Development of the Tamar River Tidal Test Facility

Tom Mitchell Ferguson#1, Irene Penesis#2, Rowan Frost#3, Keyvan Sartipi#4, Nathan Kemp#5, Jean-Roch Nader#6,
Remo Cossu*7

#*National Centre for Maritime Engineering and Hydrodynamics, Australian Maritime College, University of Tasmania*
1thomas.mitchellferguson@utas.edu.au
2i.penesis@utas.edu.au
3rowan.frost@utas.edu.au
4kevin.sartipi@utas.edu.au
5nathan.kemp@utas.edu.au
6jeanroch.nader@utas.edu.au
**Faculty of Engineering, Architecture and Information Technology, The University of Queensland, Australia*
7r.cossu@uq.edu.au

***Abstract*—Performing full scale field testing is a key stage in developing a tidal turbine. This generally occurs during Technical Readiness Levels (TRL) 6-9 and is associated with difficulty in attracting funding and large one off capital costs without an associated income stream. It therefore poses a large obstacle in the development of commercially-ready devices. The advancement of purpose built test facilities such as the European Marine Energy Centre (EMEC) can substantially reduce risks and costs to technology developers by providing berths with foundations and moorings, site characterisation and vessels for deployment support. This paper presents the development of a tidal test facility in the Tamar River estuary in Tasmania, Australia. The process for site identification, site characterisation including bathymetry and mooring design are detailed and ADCP velocity profiles for the low flow site are presented. Key findings from the work performed included requiring a strong understanding of environmental parameters in restricted water such as estuaries and the challenges in designing cost effective tidal mooring systems due to the lack of sediment present at highly energetic sites. Further development at the high flow sites includes the use of a purpose built test barge and grid connection.**

***Keywords*— Tidal energy; test site; site characterisation; mooring design; tidal turbine**

I. INTRODUCTION

Australia is home to some of the largest tides in the world, with a mean tidal stream energy density of between 600 and 2000 W/m^2 in the Banks Strait in southern Australia [1]. Several prospective sites for tidal energy exist in Australian shelf waters, including in both locations near to demand (Northern Territory Electricity Network) or the National Electricity Market, and remote locations able to serve remote communities. Some potential sites shown in FIG. 1 include: King Sound, WA (total resource ~13 TWh/yr), Clarence and Dundas Straits, NT (~12 TWh/yr), Torres Strait, Qld (~4.5 TWh/yr), and Banks Strait, Tasmania (~3 TWh/yr) [2].

With thus far unexploited resources, many Australian-based tidal energy companies including established companies MAKO Tidal Turbines and BioPower Systems, early level developers Cetus and InfraTidal, as well as offshore consultancy companies such as Advisian (Worley Parsons Group) are keen to expand into ocean renewable energy [3].

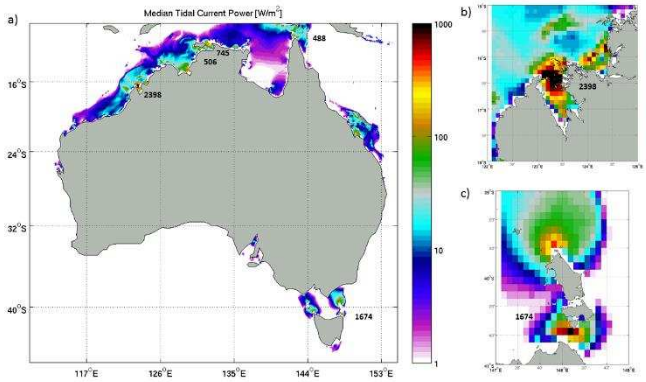

Fig. 1 Median tidal current power according to the National Tidal Centre tidal model used in the CSIRO 2012 Ocean Energy Report [2]. a) National; b) King Sound (NE Australia); c) Banks Strait (SE Australia)

In addition, the Australian Renewable Energy Agency (ARENA) has recently announced funding for two tidal energy projects; a feasibility study into Advisian's Tidal Turbine Reef (TTR) project [4], and a tidal resource and feasibility study led by the Australian Maritime College (AMC) in collaboration with the CSIRO and The University of Queensland [5]. This 3-year project, supported by industry partners, OpenHydro, MAKO Tidal Turbines, BioPower Systems and Protean Wave Enegy, will create an online atlas mapping Australia's tidal energy to the nearest 500 meters, and a full feasibility study of two high potential sites including the modelling existing tidal energy devices at these sites. The outcomes from this project will be of commercial value to any tidal company wishing to deploy their technology in the most energetic tidal sites in Australia.

A key stage in the development of a tidal energy device occurs during Technical Readiness Levels (TRL [6]) 6-9 during technology demonstration [7]. This challenging period is known as the "valley of death" as many companies struggle to attract sufficient funding to finance the increased expenses associated with demonstrating and field testing technology. Prior to collaborating with MAKO Tidal Turbines to deploy their technology in the Tamar River in 2016 only one other full scale tidal turbine had been field tested in situ within Australia, Atlantis Resources 150 kW Nereus turbine at San Remo, Victoria in 2008 [8].

Many of the costs associated with demonstrating technology are one off costs associated with developing a test site [9] such as developing berths with moorings, foundations, platforms (for floating concepts), grid connections, site characterisation, environmental monitoring, deployment equipment and vessels and permitting. This process is expensive and time consuming yet does little to advance the technology itself resulting in difficultly in attracting investment and reducing risk. The development of test sites such as those developed by EMEC [10] allow these costs to be reduced and therefore improves outcomes for tidal energy companies.

During the early stages of full scale testing it can be valuable for companies to place their devices at sites with lower flow speeds. Low flow sites provide an area for rehearsals of deployment techniques, device components to be tested for reliability such as the power take-off systems and communication systems, and other environmental factors such as the impact of biofouling to be examined. This initial testing stage allows companies to gain a stronger understanding of their turbines operation and identify potential failures prior to exposing the turbine to a highly energetic tidal stream where small failures can be amplified. In many cases it will reduce the risk and overall costs associated with developing their technology.

Testing at low flow sites can also allow the investigation of interactions between tidal devices and marine animals and/or local habitats, which are still not well known. For instance, potentially high risk interactions include; i) collision of animals with tidal turbines; ii) underwater noise from marine renewable energy (MRE) devices on animals; iii) electromagnetic fields (EMF) from cables and devices; and iv) changes in benthic habitats and reefing of fish, due to MRE devices [11]. Some guidelines have recently been introduced [11, 12] to monitor the environmental impact of MRE and provide an environmental statement (ES).

Large research institutions are able to contribute to the development of field site testing facilities as they often have access to critical resources at costs below commercial rates often set for offshore oil and gas companies. The University of Tasmania's (UTAS) Australian Maritime College (AMC) has access to a wide range of infrastructure which is required for the development of a test site. This includes: multiple vessels ranging from a 35 m fisheries training vessel to small dinghies, port facilities for the launch and recovery of turbines, multiple Autonomous Underwater Vehicles (AUVs) for capturing bathymetry and sub-bottom information and field instruments (current profilers, turbulence probes, CTDs, etc.) for site characterisation.

This paper will present the work undertaken to develop the Tamar River Tidal Test Facility in Tasmania, Australia which consists of three sites; two high flow sites for bottom mounted and floating turbines with a maximum flow velocity of approximately 2.50 m/s and a low flow site with maximum flow velocity of approximately 1.50 m/s. The following key stages are highlighted including:

- site selection;
- field measurements;
- data processing and site characterisation; and
- mooring design.

II. TAMAR RIVER ESTUARY

The Tamar River estuary (Fig. 2) is located on the Northern coast of Tasmania and stretches 70 km between the merging of the North and South Esk Rivers and its mouth at Low Head. The estuary is primarily used for shipping, aquaculture and recreational uses.

The river experiences semidiurnal tides with a tidal range of approximately 3 m occurring every 12 hours [13]. A key location within the estuary is the Batman Narrows where the river constricts from a width of 900 m to only 225 m resulting in high velocity flows.

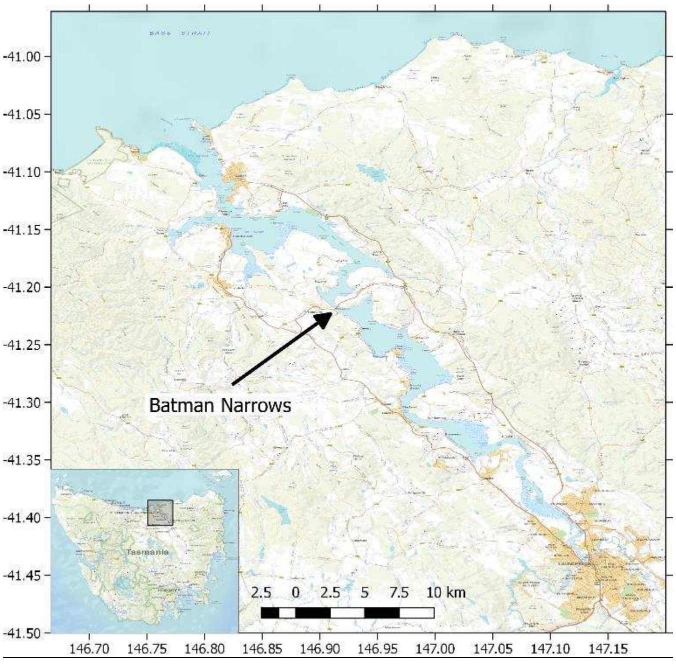

Fig. 2 Tamar River estuary including the location of the Batman Narrows where the River narrows from a width of 900 m to 225 m

The bottom mounted high flow site has been studied extensively by Green *et al.* [14] who determined that the maximum flow at the centre of the constriction was approximately 2.45 and 2.54 m/s on the flood and ebb, respectively. However due regulatory requirements, in this case the presence of the shipping channel, this location is only suitable for situating a bottom mounted turbine and other locations outside of the shipping channel must be considered for floating designs.

III. METHODOLOGY

A. Bathymetry

Detailed bathymetry around the low flow site was collected using AMC's Gavia class AUV equipped with a Kongsberg GeoSwath+ interferometric sonar and a Kearfott T-24 Inertial Navigation System (INS) for improved navigational accuracy. The GeoSwath+ has a depth resolution of 1.5mm and the INS has an accuracy of ±0.1% of the distance travelled since the last GPS fix (surfaced). The horizontal spatial resolution was 0.25 m. During the AUV survey a tide gauge was measuring the tide height and a Conductivity-Temperature-Depth (CTD) cast was conducted to allow the calculation of sound velocity through the water to correct the sonar data. The AUV was limited in its ability to gather data close to the extremely shallow water at Reid Rock.

B. Flow measurements

Detailed site characterisation at the low flow site was performed using a static bottom mounted Teledyne Workhorse Sentinel V50 Acoustic Doppler Current Profiler (ADCP). The ADCP utilises the Doppler Effect to measure flow velocity at a number of points throughout the water column allowing the full velocity profile to be measured. The setup parameters of the ADCP are shown in Table I.

TABLE I
ADCP DEPLOYMENT SETUP PARAMETERS

Parameter	Value	Unit
Ping rate	0.067	Hz
Pings per ensemble	15	
Ensemble time	300	s
Bin size	0.5	m
Blanking distance	1	m
Mean depth	18.0 ± tide	m

The ADCP was mounted to a steel frame with dimensions of 1800x1050x750 mm and weight of approximately 350 kg including 210 kg of additional ballast. The frame was attached to an L-shaped mooring to ensure the mooring line did not impact upon the data collected (Fig. 3).

The frame was constructed of a 30 m length of lead core tethered to 230 kg train wheel, which is subsequently attached to nylon line connected to a large yellow surface marker. The large train wheel is necessary to ensure the surface marker does not drag on the seabed.

Fig. 3 The steel frame housing the ADCP attached to L-shaped mooring (not to scale)

The frame and instruments were installed using the AMC vessel *Reviresco* on the 11th of November, 2017 for an anticpated deployment of 42 days. Unfortunately equipment failure resulted in a reduced capture period of 13 days. The tidal elevation during this period is shown in Fig. 4. This period includes the largest spring tide of the year occurring on November 18th.

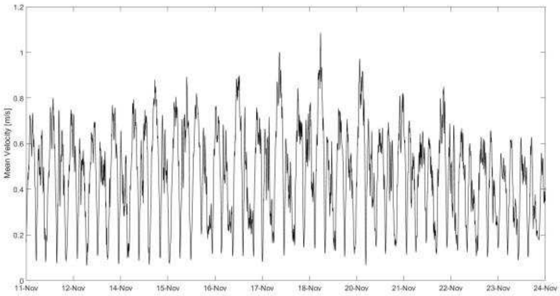

Fig. 4 Mean velocity during the deployment of the ADCP at the low flow test site showing the spring tide occurring on November 18

The magnitude of the horizontal component of the flow is the used to calculate flow velocities:

$$V = \sqrt{u^2 + v^2} \qquad (1)$$

Where V is the horizontal flow magnitude [m/s], u is the north-south component of velocity [m/s] and v is the east-west component of velocity [m/s]. Due to the nature of field experiments and the use of Doppler based measurement devices, outliers and noise are always present in data collected. To reduce the impact of these factors, prior to any investigation was performed a 3 point moving average filter was performed [14].

The power density at the site is determined by calculating the kinetic energy present within the flow using [15]:

$$P = \frac{1}{2}\rho V^3 \qquad (2)$$

Where P is the power density [W/m^2], ρ is water density [kg/m^3] and V is the water velocity [m/s].

IV. SITE SELECTION

To establish possible initial sites for the tidal test facility a vessel mounted Sontek MicroADV was utilised at a wide range of locations within the estuary. The vessel was anchored at prospective locations while the velocity was recorded before relocating to the next site. The MicroADV has a resolution of 0.1mm/s and was set to record at 50Hz or 10Hz for the longer sample times.

The key criteria for identifying possible locations included:

- high flow velocity;
- consistency between flood and ebb velocity;
- sufficient swing room for a vessel of 15 m length, 5 m draft;
- does not obstruct shipping or other users of the river
- water depth of less than 20 m.

Flow was measured at 34 locations throughout the estuary over varying sample times shown in Fig. 5.

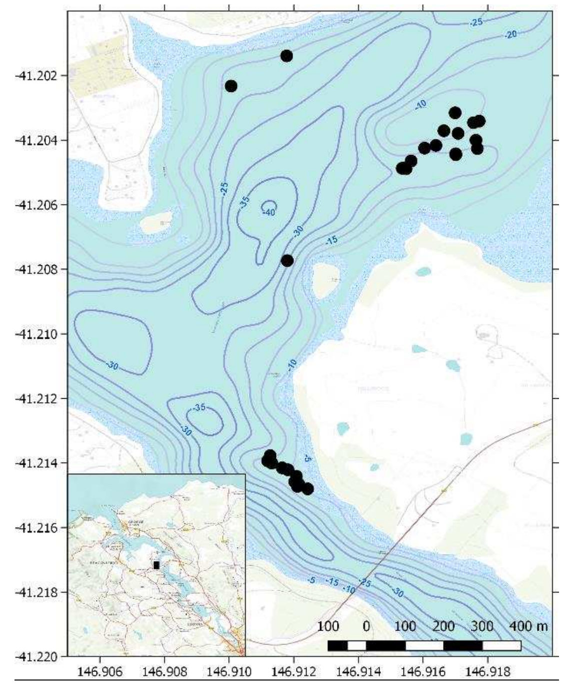

Fig. 5 The 34 sites investigated using the vessel mounted ADV. Particular focus was placed on locations in close proximity to features such as rocks or shallow water.

In addition to the high flow site already investigated [14], two additional sites were identified for further investigation; a low flow site with a targeted maximum flow velocity of 1.5 m/s, and a high flow site with an anticipated maximum flow velocity of 2.5 m/s. Thus prior to installation, an initial assessment on the biotope and habitat mapping of the proposed test site was completed; bird and fish species, mammals, seafloor substrate, and benthic assessment was completed by reviewing video captured using a series of drop cam tracks.

Imagery was recorded on a GoPro set to 1920*1080 resolution at 30 frames per second. The drop cam was lowered while the surface vessel was allowed to drift freely with the current. The drop cam track lines were recorded from surface vessel with a Garmin (GPS18X) GPS.

The benthic assessment found low macro invertebrate presence and diversity at the site, except for a small area of high sponge diversity was observed at the southern end of the site, which was subsequently avoided. Large fauna within the river include seals attracted to the nearby aquaculture farms. In addition, the estuary is a known breeding area and nursery for grey nurse sharks. The substrate was of two general types; exposed rocky reef, and unconsolidated, unvegetated course-grain sand mixed with shell or gravel.

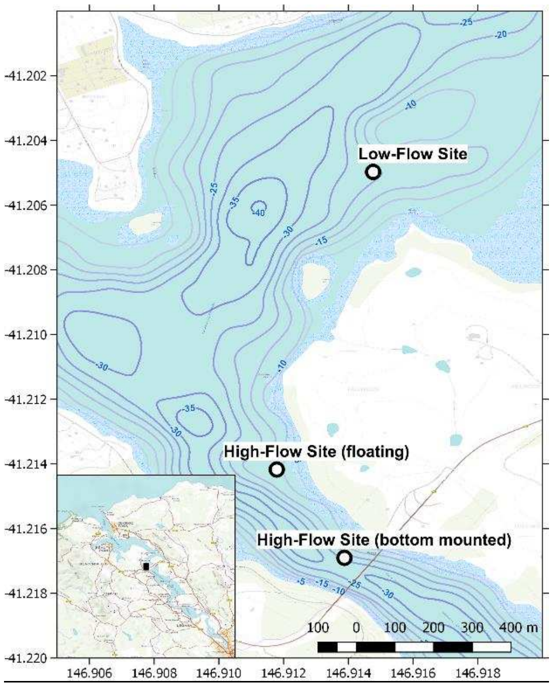

Fig. 6 High and low flow sites identified within the Tamar River estuary

A. Low Flow Test Site

The low flow site is situated approximately 0.8 nautical miles north of the Batman Narrows in close vicinity to Reid Rock. This feature, which is exposed at low tide, results in the river splitting into two channels, the main shipping channel passing north of the Rock and a secondary channel passing south. While the low flow site was situated outside of the main channel it was anticipated that the accelerated flow around Reid Rock would result in higher flow velocities at the site. As this site is located on a bend in the river a higher velocity on the flood than on the ebb tide was anticipated.

The bathymetry, shown in Fig. 7 revealed a relatively flat channel running south of the rock with a depth of approximately 20 m. There is a sharp incline to the north of the site at Reid Rock which extends from the exposed rock directly north to shallow water north east of the site.

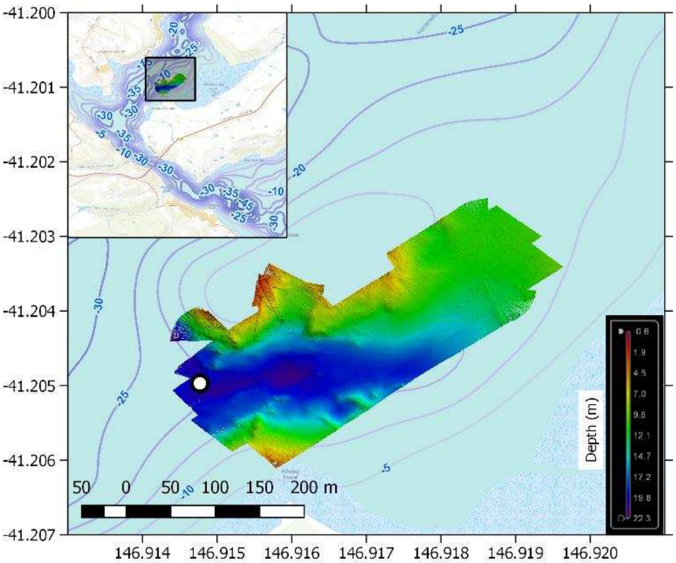

Fig. 7 Bathymetry surrounding the low flow site overlayed on available charts showing the channel running south of Reid Rock with the site located in 18 m water depth

Bottom grabs performed at the site failed to capture any sediment. Following this, a drop cam was used to investigate the seafloor. A lack of light resulted in no vision being captured at depths greater than 12 m. However, where suitable video was captured the seafloor consisted of a hard rock substrate with some boulders – typical of most high energy tidal sites.

B. *High Flow Test Sites*

The high flow sites are located at the Batman Narrows. Bathymetry (Fig. 7 and 8) was captured at the high flow site using the same method as detailed for the low flow site. The site sits on a ledge with water depth of approximately 12 m, while the bottom mounted site sits on a ledge of approximately 18 m. The channel runs east of the site with the water depth reaching 40 m after a sharp drop from the ledge.

Previous studies [14] performed at the bottom mounted site found maximum flow speeds in excess of 2.50 m/s. Based on the investigations performed using the vessel mounted ADV it is anticipated that the high flow site will match these flow speeds.

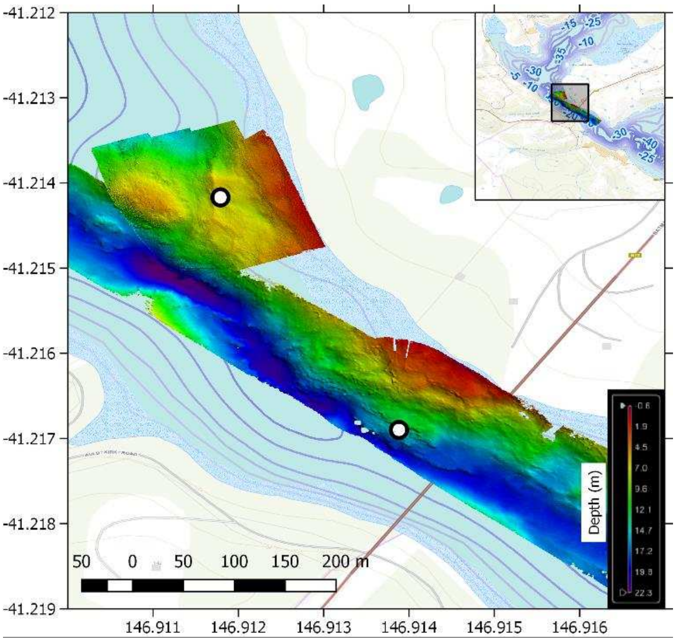

Fig. 8 Bathymetry surrounding the floating and bottom mounted high flow site overlayed on available charts showing the floating mooring sitting in approximately 12 m water depth and bottom mounted mooring sitting in approximately 18 m water depth

V. SITE CHARACTERISATION

A summary of the findings from the low flow site are presented in Table II alongside the previous study performed at the high flow site [14]. During the 13 day deployment a maximum velocity of 1.4 m/s was recorded during a flood. Due to the presence of the spring time during this period it is likely that this is very close to the maximum velocity that will be experienced at the site. This is close to the targeted 1.5 m/s maximum velocity. The reduced measurement period likely resulted in a slightly higher estimation of the mean velocity as it failed to fully capture a neap tide (early November 11th and November 25th). Both the mean and maximum velocity was lower on the ebb than during the flood.

For some turbines designs the presence of unsymmetrical flow direction and magnitude between flood and ebb can result in efficiency losses in one or both directions due to the turbine requiring to operate efficiently across a wide range of velocities. Therefore symmetry in both direction and magnitude is important to maximise turbine efficiency. The low flow site provided a 186.16 degree difference in the principle axis of the flood and ebb direction.

The high flow site [14] provides a significantly more energetic and symmetrical flow. It provides approximately 2.5 times the power density of the low flow site on the flood and 4 times the power density on the ebb.

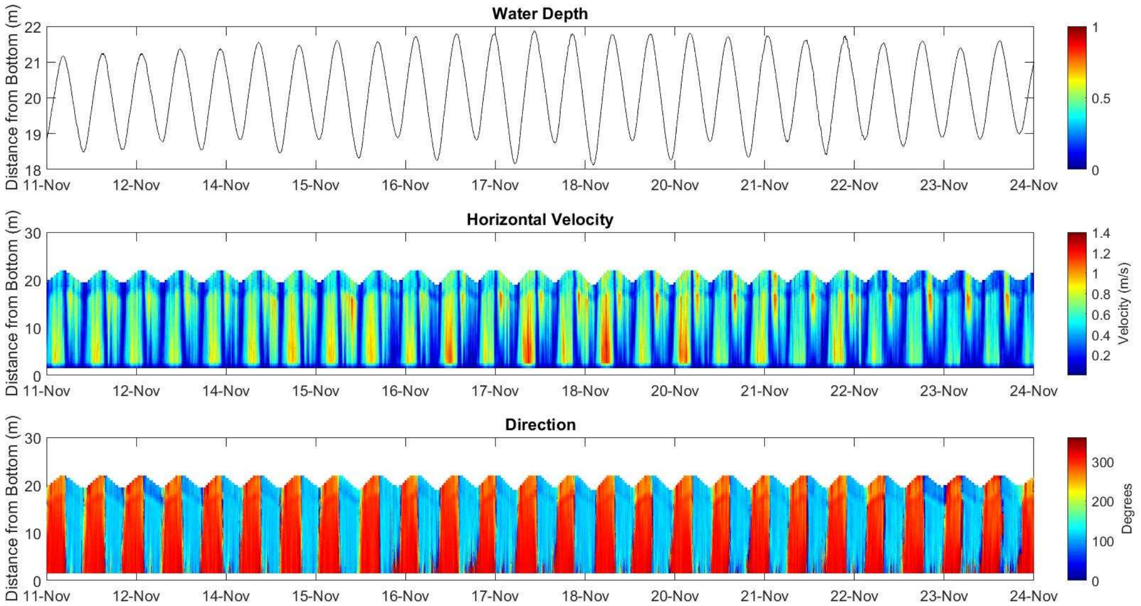

Fig. 9 a) The tidal elevation during the measurement period which includes the spring tide occurring on November 18th. b) The horizontal water velocity during the measurement period. The higher flows present during the spring flood tides can be seen on Nov 18th. c) The directionality of the flow throughout the water column

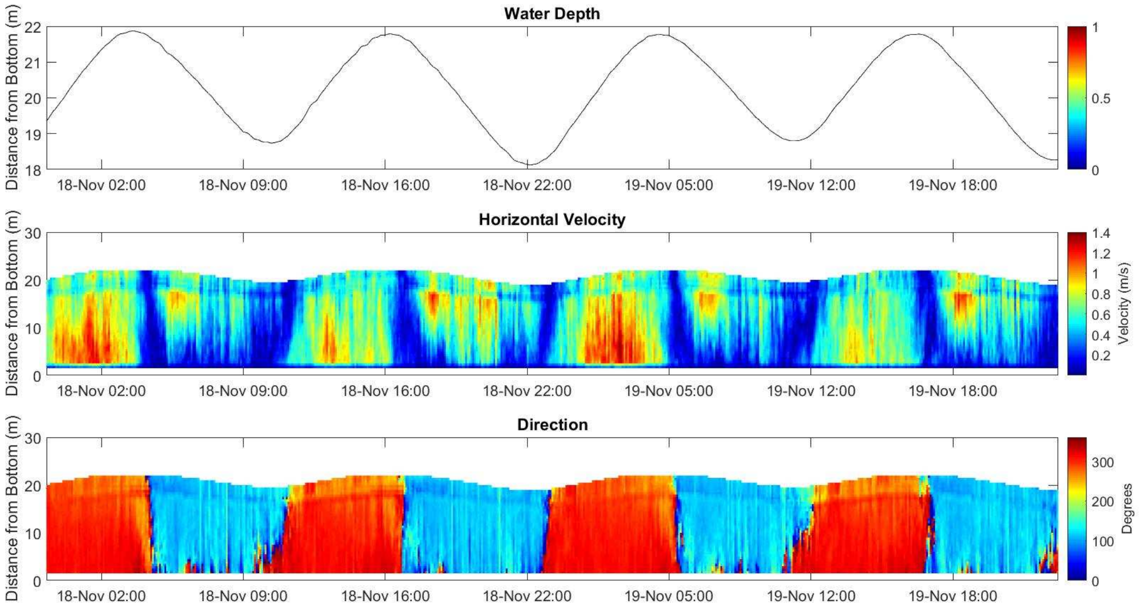

Fig. 10 a) The water depth during the spring tide occurring on the 18th of November. b) The horizontal water velocity during the spring tide occurring on the 18th of November, highlighting the differing flow direction through the water column occurring at low tide. c) The directionality of the flow throughout the water column

TABLE II
SUMMARY OF MEASUREMENTS AT THE HIGH [14] AND LOW FLOW SITE

	Low Flow site		**High Flow site [14]**		
Parameter	**Flood**	**Ebb**	**Flood**	**Ebb**	**Unit**
Velocity					
Maximum velocity	1.40	1.24	2.45	2.54	m/s
Mean velocity	1.13	0.92	1.55	1.47	m/s
Vertical Profile					
Power law exponent	7.49	1.27	10.4	2.02	
Standard deviation	0.038	0.016	6.252	0.279	
Directionality					
Principle axis	110.14	296.31	85.47	265.51	degrees
Standard deviation	23.73	23.28	5.94	5.92	degrees
Ebb/Flood asymmetry	186.16		178.04		degrees
Power					
Mean power density	0.733	0.403	1.91	1.63	kW/m^2

The water depth, horizontal velocity and horizontal direction measured are shown in Fig. 9. This period included the largest spring tide of the year occurring on the 18th of November, this can clearly be seen in the presentation of the horizontal velocity (as the large red areas).

Fig. 10 shows more detail of the time around the spring tide. There are two key areas which should be highlighted. The first is the inconsistent velocity shown by vertical blue stripes, this is particularly prevalent during the ebb. These could possibly be caused by large eddy structures passing down the river however further studies would need to be undertaken to further investigate this.

The second phenomena occurs during the transitions between ebb and flood. At low tide it can been seen that the velocity at the bottom of the water column transitions to flood significantly earlier than that at the water surface. This can be seen in both the velocity magnitude and direction plots. This effect is not present at high tide during the transition from flood to ebb. While this figure shows the period around the spring tide these phenomena occurred throughout the measurement period.

Boundary layer formation and free surface effects can have a major effect on the vertical profile of the horizontal velocities. There are a number of methods for estimating the impact of the boundary layer upon the flow speed through the water column, however it is generally recommended that the profile be modelled using the 1/10th power law [15]:

$$V = V_0\left(\frac{z}{d}\right)^{1/\alpha} \tag{2}$$

Where V is the horizontal velocity [m/s], V_0 is the surface velocity [m/s], z is the depth at which the velocity is to be approximated [m], d is the water depth [m] and α is a constant determined by the boundary layer. It is recommended that an α value of 10 is used however previous studies in the area have shown that this is not suitable for this location due to turbulence and large eddies within the water column due to changes in bathymetry [14].

The presence of a boundary layer on the seafloor results in a change in the velocity throughout the water column. Generally this is modelled using a 1/10th power law [15]. Fig. 11 presents the velocity profile at the low flow site during a typical ebb and flood tide, grey areas indicate regions in which the flow is likely to be effected by wind and waves resulting in poor correlation and is therefore unreliable [14]. Also shown is a curve fitted using the least squares error method to Eq. 2 to determine the value for α. The curve was only fitted to the region in which reliable data was gathered. Typical values for α vary between 7 and 10, however for the ebb a value of 1.27 is determined. This indicates a slow transition to the maximum velocity occurring near the surface. The reduction in velocity at the surface can be caused by many factors including surface friction and wind shear and is typical in wide rivers with a large width/depth ratio. While not typical this is consistent with previous findings in the estuary by Green et al. [14] who determined an α value during ebb of 2.02 at the Batman Narrows. It is possible this is caused by the large constriction prior to the low flow test site resulting in disturbed flow and therefore impacting on boundary layer creation. Bed roughness can also result in a sub-layer which can shift the profile vertically. An α value of 7.49 was determined during the flood which indicates thin boundary layer effect.

Detailed velocity profiles from the high flow site can be found in [14]. A detailed site characterisation has not yet been performed at the floating high flow site determined in Section III (B).

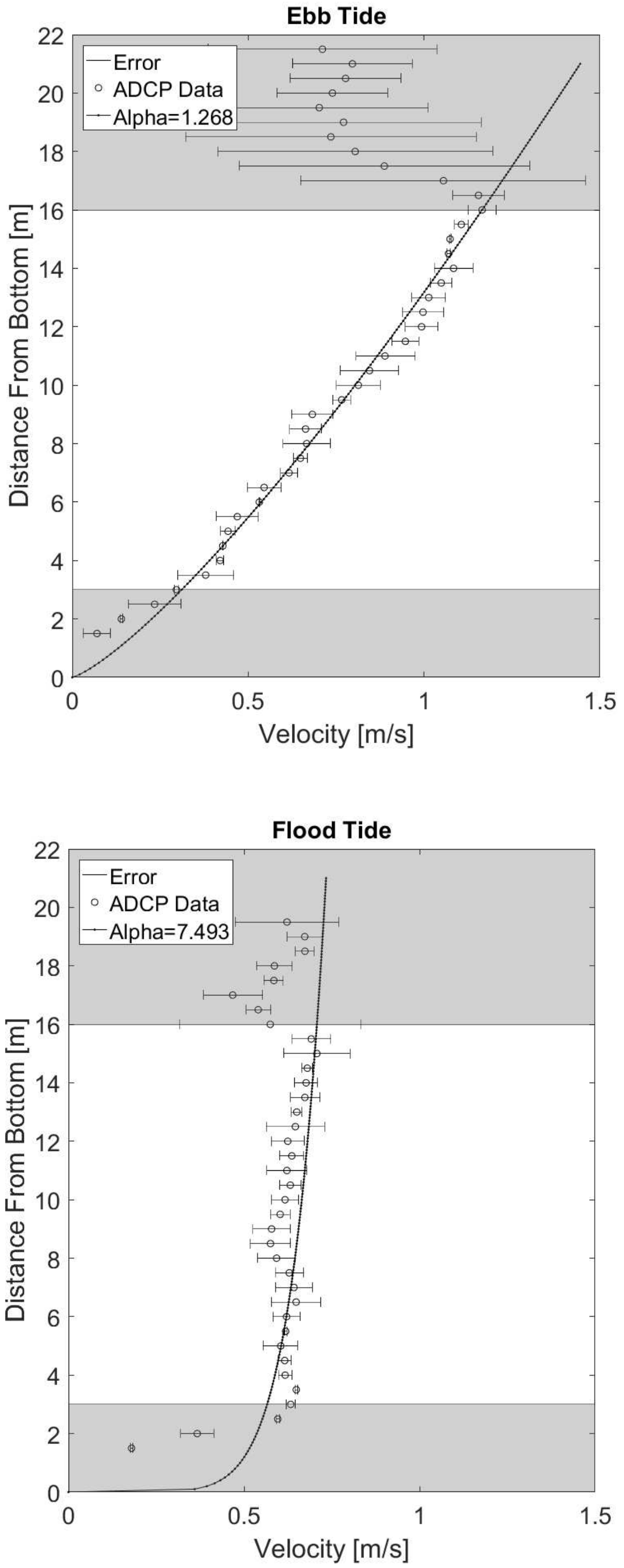

Fig. 11 Typical velocity profile at the low flow site during a typical a) ebb and b) flood tide showing a power law fit. Grey areas represent regions of increased uncertainty due wind and wave effects

VI. MOORING DESIGN

Due to time and cost constraints the guiding principle behind the design of the mooring was simplicity, in particular focussing on materials and infrastructure we were able to source locally.

Bottom grabs and drop cam footage showed the sea floor consisted of hard rock with some small boulders. Importantly there was a complete lack of sediment. This immediately eliminated many common anchoring solutions such as embedment or suction anchors. Due to the timeframe, it was not feasible to conduct the level of geotechnical survey required for pile or screw type designs therefore a gravity anchoring solution was adopted.

Mooring loadings were calculated according to BS6349 [16] with an additional loading for the turbine which could be calculated using an actuated disk model assuming a peak value for the induction factor [17]. The major challenges encountered during the design process were to ensure sufficient strength in the mooring to withstand the loadings generated by the turbine, reduce the swing room to less than 45 m and minimise the vertical loading placed upon the turbine barge. A factor of safety of 1.5 was applied to the mass of the clump weight and a factor of safety of 3 was applied to all lengths of chain and associated fittings [16].

Fig. 12 Mooring clump weigh and lengths of 50 mm grade 2 black studless chain prior to installation at the low flow site

The mooring consists of:

- One 5.1 t cast iron clump weight encased in 6 mm thick outward facing tread plate with an additional 3.2 m of 50 mm grade 2 black studless chain for a total weight of 5.27 t and 4.51 t in air and in water respectively (Fig. 12).
- A bridle composed of two 3 m lengths of 50 mm grade 2 black studless chain.
- Two lengths of 10 m 50 mm grade 2 black studless chain.
- Two lengths of 6 m 16 mm grade L galvanised studless chain.
- 13.5 m of 32 mm three strand polypropylene rope.
- 1.5 m of 32 mm three strand polypropylene rope.
- two large floats when not attached to test barge.

A catenary is the shape a chain makes when suspended under its own weight. A first principles approach was adopted to determine the catenary profile and therefore the moorings swing room. At full load, it is anticipated that the mooring will be under 1.9 tonne of tension and have a swing room of 43.6 m. The catenary will place a horizontal load of 1.6 tonne and vertical load of 1.1 tonne on the barge.

The mooring has subsequently been utilised by MAKO Tidal Turbines [18] who, in collaboration with AMC, have completed a six month trial of their 2.5 m sweep diameter tidal turbine on the mooring between October 2016 and April 2017 (Fig. 13). While the mooring was not instrumented during site visits it was observed that the mooring successfully held the barge within the required swing room. The barge was stable during operations and held the turbine into the flow.

It is clear that mooring design will need to be a key area of focus for the high flow site as the increased loadings placed on the mooring will make installation of a gravity mooring significantly more challenging due to the increased weight of the mooring and the availability of a vessel which is able to navigate in the restricted waters of the estuary while still having a suitable lifting capacity. This may require the use of multiple clump weights tied to a single mooring or the investigation of other anchoring concepts such as screw types [19]. This challenge is not unique to the Tamar River estuary and will need to be overcome to reduce high costs of anchoring for marine energy devices.

VII. CONCLUSIONS

Development of the low flow site was considered successful with the process identifying a suitable site, characterisation performed and mooring installed. The measured maximum flow velocity reached 1.40 m/s. Two further sites with higher flow velocities are being developed for floating and bottom mounted devices. Both of these sites are expected to have a maximum velocity of approximately 2.50 m/s. The development is anticipated to include a purpose build test barge and grid connectivity.

Analysis of the flow data gathered through the development process identified some characteristics generated by the constricted nature of an estuary, bed roughness and rapid depth changes which are not typical in open waters, which can result in changes to the velocity profile though the water column and the presence of large eddy structures.

Developing cost effective moorings will provide an on-going challenge for the tidal energy sector as locations with high current flows are unlikely to have significant sediment in addition to high horizontal loadings place significant limitations on the mooring concepts which are suitable. Significant progress in this area will be required to reduce costs for tidal energy companies.

The successful development of the Tamar River tidal test facility will complement and support current tidal energy projects funded by ARENA and enable tidal developers to test and evaluate their turbines within Australia in a well-understood environment at a significantly reduced cost, assisting them in progressing their technology towards commercialisation.

Fig. 13 The operational MAKO Turbines test barge attached to the low flow mooring

VIII. ACKNOWLEDGEMENTS

The authors would like to acknowledge the collaboration and assistance provided by Tyrone Misselhorn, MAKO Tidal Turbines, TasPorts, Marine and Safety Tasmania, NRM North, AMCSearch and the technical staff at AMC's Beauty Point campus.

IX. REFERENCES

1. Rahimi, R., I. Penesis, M. Hemer, L. Mason, and G. Thomas, *Characterization of the tidal current resource in Tasmania.* Renewable Energy, 2014. **2015**: p. 2050.
2. Behrens, S., D. Griffin, J. Hayward, M. Hemer, C. Knight, S. McGarry, P. Osman, and J. Wright, *Ocean Renewable Energy: 2015-2050: An analysis of ocean energy in Australia*. 2012: North Ryde.
3. Hemer, M., R. Manasseh, K. McInnes, I. Penesis, and T. Pitma, *Perspectives on a Way Forward for Ocean Renewable Energy in Australia.* Renewable & Sustainable Energy Reviews (Under review), 2017.

4. Australian renewable Energy Agency (ARENA). *Tidal Turbine Reef Feasibility Study*. 2017; Available from: https://arena.gov.au/projects/tidal-turbine-reef-feasibility-study/
5. Australian Renewable Energy Agency (ARENA). *Tidal Energy in Australia – Assessing Resource and Feasibility to Australia's Future Energy Mix*. 2017; Available from: https://arena.gov.au/projects/tidal-energy-australia-assessing-resource-feasibility-australias-future-energy-mix/.
6. Mankins, J.C., *Technology readiness levels.* 1995.
7. Johnston, K.E., I. Penesis, and R. Rahimi, *Investigating the development of large scale wave converter test sites in Tasmania*, in *3rd Asian Wave and Tidal Energy Conference*. 2016: Singapore.
8. Atlantis Resources Ltd. *Technology History*. 2017; Available from: https://www.atlantisresourcesltd.com/services/turbines/history/.
9. Holmes, B. and K. Nielsen, *OES-IA Annex Task 2.1, Report T02-2.1, Guidelines for the Development and Testing of Wave Energy Systems*. 2010.
10. European Marine Energy Centre Ltd. *Grid-connected tidal test site*. 2017; Available from: http://www.emec.org.uk/facilities/tidal-test-site/.
11. Copping, A., N. Sather, L. Hanna, J. Whiting, G. Zydlewski, G. Staines, A. Gill, I. Hutchison, A. O'Hagan, T. Simas, J. Bald, S. C., J. Wood, and E. Masden, *Annex IV 2016 State of the Science Report: Environmental Effects of Marine Renewable Energy Development Around the World*. 2016.
12. European Marine Energy Centre Ltd, *Environmental impact assessment (EIA) guidance for developers at the European Marine Energy Centre*. 2005.
13. Australian Bureau of Meteorology. *2017 Times and Heights of High and Low Waters for Bell Bay, Tasmania*. 2017; Available from: http://www.bom.gov.au/ntc/IDO59001/IDO59001_2017_TAS_TP016.pdf.
14. Green, S., R. Cossu, I. Penesis, and J.-R. Nader, *Tidal Energy: A Promising Future Resource for Tasmania*, in *3rd Asian Wave and Tidal Energy Conference*. 2016: Singapore.
15. European Marine Energy Centre Ltd, *Assessment of Tidal Energy Resource*. 2009: London, United Kingdom.
16. British Standard, *BS 6349-6:1989 "Code of practice for Maritime structures — Part 6: Design of inshore moorings and floating structures",*. 1989.
17. Masters, I., J. Chapman, M. Willis, and J. Orme, *A robust blade element momentum theory model for tidal stream turbines including tip and hub loss corrections.* Journal of Marine Engineering & Technology, 2011. **10**(1): p. 25-35.
18. MAKO Tidal Turbines Pty Ltd. *Turbine Demonstration Project - Tasmania*. 2017; Available from: https://mako.energy/projects/tamar-river-research-project.
19. tidalenergytoday. *MSE, SME conclude 'SAMED' project*. 2015; Available from: http://tidalenergytoday.com/2015/04/01/mse-sme-conclude-samed-project/.